On the exceptional time-on-stream stability of HZSM-12 zeolite: relation between zeolite pore structure and activity

Wenmin Zhang and Panagiotis G. Smirniotis *

Department of Chemical Engineering, University of Cincinnati, Cincinnati, OH 45221-0171, USA
E-mail: Panagiotis.Smirniotis@uc.edu

Received 9 December 1998; accepted 18 May 1999

ZSM-12 and several other 12-membered ring large-pore zeolites have been tested for the reforming of naphthenic hydrocarbon mixtures. It was found that ZSM-12 possesses a surprisingly higher coking resistance than other large pore zeolites tested such as USY, L-zeolite, mordenite, and β-zeolite for reforming of hydrocarbon mixtures. This superior performance is due to the unique non-interconnecting tubular-like linear channels of ZSM-12, which do not allow trapping/accumulation of coking precursors. ZSM-12 zeolite also demonstrated excellent structural stability even under severe acid dealumination. From this work, we found that the decrease of the aluminum content of a zeolite is not sufficient to ensure low rates of coke deposition. We also concluded that zeolites with channel intersections (cavities) of comparable size with the zeolite apertures do not favor coke formation. For these types of zeolites the strong acid sites carry out other acid-catalyzed reactions, rather than forming coke. In contrast, zeolites with relatively large supercages are inherently favorable to coking reactions, which in turn lead to the fast deactivation. The appropriate combination of the zeolite pore structure and acidity (controlled via dealumination) showed superior TOS behavior (time-stable activity and product selectivities). For zeolites which are susceptible to coking due to pore structure, the increase of the Brønsted acid strength results in fast deactivation. Contrary to what one would commonly expect and previous reports, we found that one-dimensional zeolites, such as, ZSM-12, can exhibit significantly higher tolerance to coking than multidirectional zeolites.

Keywords: ZSM-12, coking resistance, acid-catalyzed reactions, time-stable catalyst

1. Introduction

The deactivation of acid zeolites in hydrocarbon reactions is generally due to the formation of carbonaceous deposits. It has been reported that those deposits are either polyaromatic at high temperatures [1–3] or paraffinic at low temperatures [4,5] in nature. This results in the plugging of the pores/channels and the covering of acid sites of the zeolites, thus decreasing the intracrystalline mass transfer and the reactivity of the catalysts. Even though the zeolite acidic properties, the nature of the reactant, and reaction temperature are important variables, the zeolite structure has been found to play a more significant role for both the deactivation rate due to coking and the composition of the carbonaceous deposits [6,7]. This is because coking is a shape-selective reaction [8]. ZSM-5 was found to be resistant to coking to a higher extent than other zeolites such as USY (ultrastable Y-zeolite) and L-zeolite [9–11]. Mordenite is an active catalyst for many applications but it deactivates very fast due to its strong acidity, which favors the undesired formation of coke. Niu et al. [11] found that if the number of the Brønsted sites is significantly larger than that of Lewis sites, the tendency of the catalysts to form coke increases. As expected, the increase of Si/Al ratio of the zeolite by dealumination can significantly increase the time-on-stream stability of zeolite catalysts [12]. However, zeolites with high silicon content are usually less active than aluminum-rich zeolites at the relatively low temperature. It is, therefore, a challenging task to develop zeolite catalysts that will possess simultaneously high catalytic activity and long operating life.

The synthesis of ZSM-12 was first disclosed in 1974 by Rosinski and Robin [13] and then others [14,15]. ZSM-12 possesses a one-dimensional non-interconnecting tubular-like channel structure (pore size 5.5×6.1 Å) [16]. It has a constraint index (CI) of 2 [17]. The spaciousness index (SI) for ZSM-12 ranges from 2.4 to 4.3 [18], and it is among the smallest 12-membered ring (MR) pore zeolites. For this reason ZSM-12 exhibited both product and transition state shape-selectivity favoring the formation of the less bulky 2-phenyl isomer for the alkylation of benzene with 1-dodecene [19].

In relation with pore structure, we report the outstanding time-on-stream behavior of ZSM-12 zeolite for acid-catalyzed reactions compared with that of other 12-MR large pore zeolites (USY, β-zeolite, L-zeolite and mordenite). A study was also conducted to discover the relationship between zeolite pore structure/acid site strength and coking tolerance in order to rationalize the catalytic performance and stability of the different zeolite catalysts.

2. Experimental

In this study, the parent ZSM-12 (Si/Al = 35) was hydrothermally synthesized from the corresponding alumi-

* To whom correspondence should be addressed.

nosilicate gels following patented literature [13]. Firstly, 2.5 g of $NaAlO_2$ was mixed with 50 g of H_2O; 40 g of tetraethylammonium bromide (TEABr) was mixed with 40 g of H_2O, and 7.0 g of NaOH was dissolved with 40 g of H_2O. Then, the above three mixtures were brought together and 200 g of Ludox (Dupont, 30% SiO_2) was added in with vigorous agitation for 2 h. The final mixtures are then moved to a sealed autoclave and kept at 140 °C under autogeneous pressure for 40 days. β-zeolite (Si/Al = 15) was synthesized in a similar way [5]. The synthesized parent zeolites were dealuminated with hydrochloric acid. Different levels of dealumination were achieved by varying the concentrations of HCl solutions. The USY samples were obtained from PQ Corporation. Steam treatment followed by severe acid leaching was involved in the synthesis of the USY-28 (CBV-760) sample. Mordenite and L-zeolites were donated to us by UOP. Ammonium hexafluorosilicate was employed for the dealumination of mordenite and L-zeolite (ammonia form). The appropriate amount of $(NH_4)_2SiF_6$ was dissolved in 200 ml H_2O, and was added dropwise within 4 h. The solution was vigorously stirred for 24 h at 90 °C. The dealuminated zeolites were subjected to ammonium exchange and calcination to obtain the protonated forms of zeolites. The loading of Pt on the catalysts (0.5 wt%) was achieved with wet impregnation of H_2PtCl_6 solution.

X-ray diffraction on a Siemens model D500 diffractometer (Cu K_α radiation) was employed for the identification of the synthesized zeolites and for the determination of the crystallinity of the dealuminated zeolites. The estimation of the crystallinity was based on the areas under the main crystallographic peaks of each zeolite. MgO was used as an internal standard for the quantitative calibration.

The catalytic experiments were carried in a flow reactor system (1/4 in. o.d. stainless-steel reactor). 100 mg of fresh catalyst were loaded on the top of a glass wool plug placed in the middle of the reactor. The catalysts were activated *in situ* by oxidation with high-purity oxygen for 1 h at 450 °C followed by purging with ultra-pure helium for 15 min. The reduction of the catalyst was carried out at 450 °C in high-purity H_2 for 1 h at atmospheric pressure. After that, the reactor temperature was increased to 470 °C and the total pressure was set at 90 psig by a backpressure regulator placed at the exit of the reactor tube. The feed mixture was then introduced into the reactor through a heated line at a predetermined flow rate using a liquid infusion pump via a special septum injection port.

NH_3 stepwise temperature-programmed desorption (NH_3-STPD) studies which were introduced earlier by us were employed [20] in order to characterize the acid sites of each zeolite (type, concentration, and strength). The STPD desorption curve consisted of five distinct desorption peaks. The five peaks occurred at the following respective temperature ranges: 150–180, 180–250, 250–350, 350–440, and 440–540 °C. The five desorption peaks from STPD were assigned to Lewis or Brønsted acid sites by utilizing FT-IR spectroscopy (BioRad FTS-40) [20,21]. Self-supported wafers approximately 3/8″ in diameter with 5 mg of H/zeolite were used for the IR measurement. FT-IR spectra were recorded at different desorption temperatures (150, 180, 250, 350, 440, and 540 °C). It is worth noting that only acidic zeolites gave this trend. The same method was applied for $DeNO_x$ catalysts made of ternary oxides ($Al_2O_3/SiO_2/TiO_2$). For these systems the number of peaks was equal to the number of ramps employed each time, and each desorption peak consisted of NH_3 desorbing from both Lewis and Brønsted sites [22]. This is not the case with acidic zeolites since the desorption profile is not sensitive to the temperature profile. For the majority of the zeolites each peak corresponds to either Lewis or Brønsted sites of different strength. This is a strong indication that zeolites possess acidic sites of distinct strength.

3. Results and discussion

3.1. Zeolite characterization

The XRD patterns of the synthesized and dealuminated ZSM-12 show a highly crystalline ZSM-12 structure [16,23]. It should be noted that ZSM-12 does not lose its crystallinity even when subjected to very severe dealumination conditions (5 N HCl solution). It is a well-crystallized sphere-shaped material with a primary particle size of about 1.0 μm and agglomerates of 3–5 μm as determined by our SEM studies. The physical properties of ZSM-12 and other zeolites are listed in table 1. Each zeolite is designated with its name followed by its bulk Si/Al ratio.

From our NH_3-STPD (table 1 and [24]) and IR studies, ZSM-12 possesses mainly low-strength Brønsted acid sites (the third desorption peak at 350 °C), which accounts for about 50% of all acid sites. This is also verified by the FT-IR spectra. From the third to the fourth desorption step, we observe a large decrease in the area of the band at 1457 cm^{-1} (NH_4^+ deformation on the Brønsted sites). The strong (ammonia desorption temperature >250 °C) to weak sites ratio (S/W) increases from ca. 2 to ca. 3 after dealumination. However, the average strong acid site strength as indicated by the *average NH_3 desorption temperature*, T_B, from strong acid sites slightly decreases (table 1). Our studies also validated that ZSM-12 and ZSM-5 samples have very similar acidic strength and acid site distribution. The mordenite possesses the highest strong/weak (S/W) acid sites ratio and thus highest number of strong acid sites. Mordenite sample with a Si/Al ratio of 36 (MOR-36) contains three times more strong acid sites than ZSM-12-35, and five times more than USY-28, though they possess comparable Si/Al ratios. The average strong acid site strength of the MOR-36 sample is also higher than those of either ZSM-12 or USY samples.

3.2. Time-on-stream behavior

A hydrocarbon mixture simulating naphthas containing 5 mol% hexane (molar percent for all compounds),

Table 1
Zeolite physical properties.

Zeolite	Dealumination agent	Si/Al (bulk)	Crystallinity (%)	T_B[a] (°C)	#NH_3/#Al	Strong/weak sites (S/W)[b]
ZSM-12-35	As synthesized	35	100	404.4	0.98	2.09
ZSM-12-54	3.0 N HCl	54	∼100	404.5	0.99	2.91
ZSM-12-69	5.0 N HCl	69	∼100	395.9	1.06	2.87
Beta-15	As synthesized	15	100	436.1	1.01	2.08
Beta-85	5.0 N HCl	85	79	439.4	0.91	2.30
USY-28[c]		28	72	409.0	0.87	1.46
MOR-36	25 g $(NH_4)_2SiF_6$	36	83	414.8	0.91	5.90
LTL-12	2.4 g $(NH_4)_2SiF_6$	12	45	397.0	0.60	1.87

[a] Average NH_3 desorption temperature from strong acid sites (NH_3 desorption temperature $>250\,^\circ$C) [24].
[b] Ratio between strong sites (NH_3 desorption temperature $>250\,^\circ$C) and weak sites (NH_3 desorption temperature $\leqslant 250\,^\circ$C).
[c] Provided by PQ Corporation (CBV-760).

10 mol% octane, 25 mol% methylcyclopentane (MCP), 25 mol% methylcyclohexane (MCH), 20 mol% propylcyclohexane (PCH), 5 mol% benzene and 10 mol% ethylbenzene was used to evaluate the coking tendency of various 12-MR large-pore zeolites. Relatively high naphthenic amounts (total 70%) and low H_2/HC ratio of 5.4 were employed in order to generate an accelerated coking environment. The conversion X and the selectivity S of the cracked products are defined as

$$X = 1 - \frac{\text{moles of unconverted reactant hydrocarbons}}{\text{moles of the reactant hydrocarbons fed into the reactor}} \times 100, \quad (1)$$

$$S = \frac{\text{moles of cracked products produced}}{\text{moles of all the products}} \times 100. \quad (2)$$

Y-faujasite has a three-dimensional pore of 7.4 Å with channel intersection (supercage) of 12 Å [25]. Mordenite consists of 12-membered ring pore channels of 7.0×6.5 Å and 8-membered ring channels of 5.7×2.6 Å, which are perpendicularly intersected with the large channels. These specific characteristics in their pore structures render both zeolites susceptible to coking by trapping (accumulation) of coking precursors. Dealuminated ultrastable Y-zeolite (USY-28, Si/Al = 28), and mordenite (MOR-36, Si/Al = 36) lost their activity rapidly with time (figure 1(a)), and a plateau was reached in about 50 h. The plateau value for the activity of USY-28 is higher than that of MOR-36. The higher plateau value as regards activity of USY-28 than that of MOR-36 was unexpected since both zeolites possess almost comparable Si/Al ratios. Based on the present results one could propose that this behavior is a result of the acidity characteristics of the zeolites. From our characterization studies we found that MOR-36 possesses stronger acid sites than USY-28 which accelerate the deactivation process (table 1). Indeed, as can be seen in table 1, the strong/weak site ratio of 5.9 for MOR-36 is much higher than that of 1.46 for USY-28. Therefore, the average acid strength is significantly greater for MOR than for USY, thus resulting in (1) the holding of coking precursors for a longer time on the surface which allows for further polymerization reactions of unsaturated intermediates, and (2) higher activity for coking reactions. Of course, the channel intersections of mordenite connecting the 12-MR with the 8-MR pores act as "stagnation" points for coke precursors, which is an

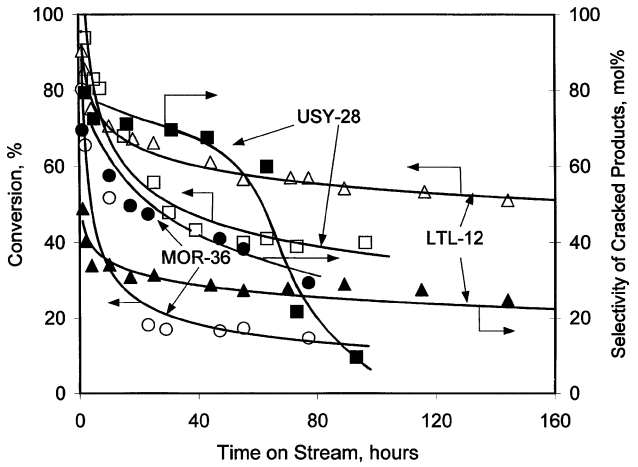

(a)

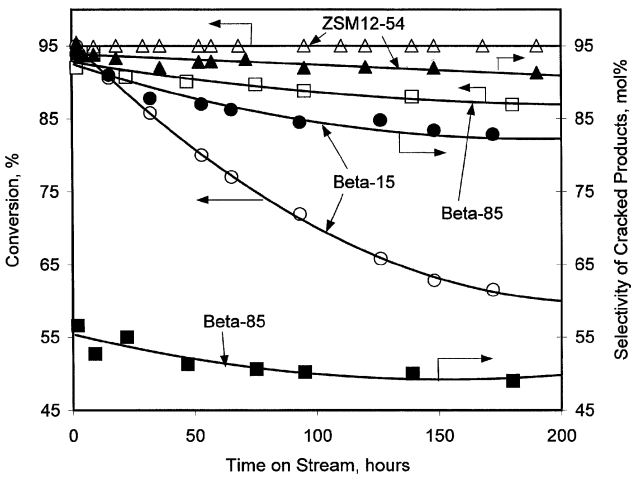

(b)

Figure 1. Time-on-stream stability and cracked product selectivity over various catalysts for the reforming of the naphthenic mixture (operating pressure 90 psig, reaction temperature = 470 °C, WHSV = 2.32 h^{-1}, H_2/oil = 5.4, Pt loading level on catalyst = 0.5 wt%). (a) USY-28, MOR-36 and LTL-12; (b) Beta-15, Beta-85 and ZSM-12-54.

additional reason for fast deactivation. The activity at the beginning of the experiments for MOR-36 is lower than that for USY-28 due to the lower Al content of the former sample.

The initial activity of L-zeolite (LTL-12) is high. However, its activity and cracking product selectivity decrease very rapidly in the initial period of 20 h, and then decrease slowly with the increase in time. This can be explained by its acid site strength distribution. From our STPD experiment, it was found that about 20% of acid sites for L-zeolite are high-strength Brønsted sites (NH_3 desorption temperature $>350\,^{\circ}C$), which deactivate rapidly during the initial period of reaction due to coke deposition. The remaining Brønsted sites (accounting for about 40% of total acid sites) are probably still available for the cracking reaction. Although LTL-12 possesses larger Al contents, the relatively higher plateau value (activity of deactivated catalyst) for LTL-12 than that for USY-28 and MOR-36 catalysts was acquired. We believe that the main reason probably responsible for this behavior is the relatively low average acid site strength of L-zeolite (table 1) which reduces the rate of deactivation.

The activity of β-zeolite decreases to a much lower extent than that of USY. The initial activity of Beta-15 is high as expected from its Si/Al ratio. However, Beta-15 loses its activity slowly with time-on-stream (figure 1(b)). In contrast to this behavior, the dealuminated β-zeolite sample (Beta-85) demonstrates significantly better time-on-stream behavior. Its activity remains unchanged for about two days on stream, and then slightly decreases with further increase in time. Compared with USY zeolite, β-zeolite demonstrates much better coking resistance, even though both zeolites have three-dimensional system of channels. The aperture size of USY is 7.4 Å, while for β-zeolite it is 7.3×6.5 Å in the a-direction and 5.6×5.6 Å in the c-direction [26]. However, the channel intersections of β-zeolite are about 10 Å, and they are smaller than those of USY, which possesses supercages of about 12 Å. Coking precursors are much more easily trapped in the supercages of USY, thus resulting in the fast deactivation of USY.

In contrast, the ZSM-12 samples show excellent time-on-stream stability in comparison with the other 12-MR large-pore zeolites studied (figure 1(b)). The as-synthesized ZSM-12 (ZSM-12-35) slightly loses its activity over a period of 100 h (not shown in the figure). Its final activity (plateau value) is higher than that of either Beta-85 or Beta-15 samples. The ZSM-12-54 catalyst is even more stable and does not lose any of its initial activity in a period of over 300 h. This exceptional behavior is consistent with our previous investigation for the reforming of industrial naphtha [5] and the hydroisomerization of n-octane [24]. This observation is in contrast to what one would expect since zeolites with two- or three-dimensional channel structures favor the efficient intracrystalline mass transfer [27], thus decreasing the possibility of pore blockage. To the best of our knowledge, our results consist of the first report that clearly demonstrate that one-dimensional zeolite ZSM-12 (with non-interconnecting uniform channels) can be a more tolerant catalyst in coke deactivation than two- or three-dimensional zeolites for the reforming or cracking reactions of paraffins and naphthenes. When the size of the aperture does not change along the length of one-dimensional zeolites, as in the case of ZSM-12, the formation of coke is hindered. ZSM-12 was reported to show better coking resistance than USY and β-zeolite in the isopropylation of benzene with propylene [28].

It is also worth noting that even though ZSM-12-54 has a lower Si/Al ratio than Beta-85, the former zeolite demonstrates superior coking resistance. In another comparison we tested under identical conditions ZSM-12-35, USY-28 and MOR-36 which have a comparable Si/Al ratio. It was found that the latter two zeolites deactivated completely within only two days, whereas ZSM-12-35 deactivates at a much lower rate. By comparing the behavior of ZSM-12-35 and ZSM-12-54, of Beta-15 and Beta-85, one can conclude that Si/Al ratio still plays a very important role. As expected, high Si zeolite possesses higher coking tolerance.

The time-on-stream selectivity of cracked products (carbon number less than seven) over ZSM-12-54 and Beta-85 does not change with time (figure 1(b)). This is a result of the relatively low rates of coke formation over their acid sites. Both mordenite and USY quickly lose their cracking ability due to the fast deactivation of the strongest acid sites followed by the deactivation of weaker sites. The only remaining reaction is aromatization which requires only less strong acidic sites. This is the typical behavior of acidic zeolites which are susceptible to fast deactivation [29]. It is worth noting that although Beta-15 gradually loses its activity (in figure 1(b)), the cracking selectivity does not decrease as much as the reaction activity. This is because of the relatively uniform deactivation of the strong, medium and weak Brønsted acid sites as was observed from our NH_3-STPD experiments for deactivated β-zeolite catalysts in our earlier work [5].

3.3. The relationship between zeolite pore structure and coking resistance

From the present data it is quite obvious that the decrease of the aluminum content of the zeolites is not sufficient to ensure low rates of coke deposition. The zeolite pore structure plays a dominant role for coking tolerance of acidic zeolite catalysts. The unique pore structure of non-interconnecting tubular-like channels (figure 2(a)) of ZSM-12 lead to its time-stable activity.

As indicated in our previous investigation [5], there are approximately two categories of zeolite pore structures with respect to the coking tolerance. The first category consists of zeolites that possess big cavities/supercages (USY and L-zeolite) or expanded channel intersections (β-zeolite and mordenite) in comparison with the main channels. Coke precursors tend to be trapped there and become large due

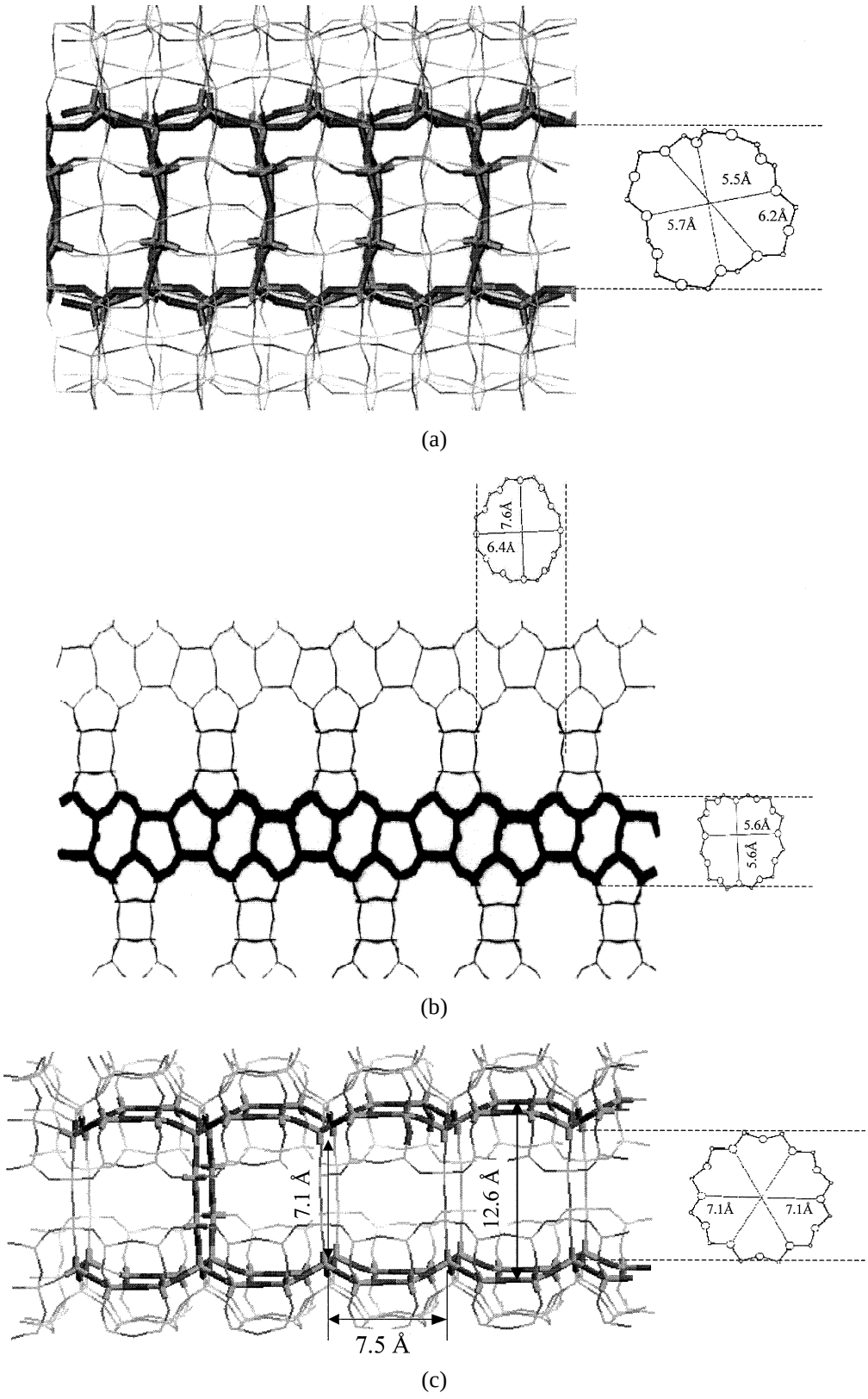

Figure 2. Pore structure of different zeolites: (a) ZSM-12, (b) β-zeolite, and (c) L-zeolite.

to polymerization reactions of those precursors, which finally block the channels and lead to catalyst deactivation. The channel intersections of β-zeolite (about 10 Å) presented in figure 2(b) are relatively smaller than those of USY (supercages of about 12 Å), which render β-zeolite to be more coke tolerant than USY zeolites. We also believe that the fast deactivation of mordenite can be attributed to the channel intersections between side-pockets and the main

12-membered ring channels. Another important reason is its strong acidity.

The second category consists of zeolites where the channel intersections for multidirectional structures are comparable with the size of the aperture (ZSM-5), or there is no periodic variation of the aperture opening along the channel of one-dimensional zeolites such as ZSM-12 (figure 2(a)). Because of these unique characteristics of the latter type of zeolites, the accumulation of coke precursors is not favored. Although L-zeolite (figure 2(c)) is also a one-dimensional zeolite, the periodic enlargement of the channel (with the biggest size of 12.6 Å and barrel length of 7.5 Å along the channels [30]) appears to play a very negative role as regards the coking tolerance of the catalyst. The large cavity of L-zeolite (12.6 Å) surrounded by the relatively small channels (7.1 Å) is the ideal place for the trapping of coking precursors, which results in the fast deactivation of L-zeolite. Ferrierite has been claimed as an excellent catalyst for the skeletal isomerization of n-butene to i-butene with long time-on-stream stability [31]. The reason for this stable behavior is that the intersections of two channels are not significantly larger than the channel sizes (4.2 $\times$ 5.4 Å and 3.5 $\times$ 4.8 Å). Other unidimensional channel materials such as ZSM-22 (4.4 $\times$ 5.5 Å) [32], ZSM-23 (4.5 $\times$ 5.2 Å) [33] and SAPO-11 (3.9 $\times$ 6.3 Å) [34] also demonstrated high stability for the above reaction.

4. Conclusions

ZSM-12 has been found to possess surprisingly higher coking resistance than other large-pore zeolites tested such as USY, L-zeolite, mordenite, and β-zeolite for the reforming types of reactions. This superior performance is due to the unique non-interconnecting tubular-like linear channels of ZSM-12, which does not allow trapping/accumulation of coking precursors. It should be noted that ZSM-12 demonstrated excellent crystal structural stability upon severe acid dealumination. Zeolites with channel intersections (cavities) of comparable size with the zeolite apertures do not favor coke formation. Zeolites with relatively large supercages are inherently favorable to coking reactions, which in turn leads to fast deactivation. Appropriate combination of the zeolite pore structure and its acidity characteristics (controlled via dealumination) showed superior time-on-stream behavior (time-stable activity and product selectivities).

With our work we found that in contrast to what is commonly believed, one-dimensional zeolites such as ZSM-12 can be significantly more stable in comparison with zeolites, which possess multidirectional pore configurations. This is a result of its specific pore characteristics which do not allow the formation of coke leading to pore plugging. For this type of zeolites, the strong acid sites are utilized in acid-catalyzed reactions other than those forming coke.

Acknowledgement

The authors wish to acknowledge the support of National Science Foundation through the CAREER Award (CTS-9702081). Acknowledgement is made to the donors of The Petroleum Research Fund, administered by the ACS, for support of this research through the grant ACS-PRF 31606-G5.

References

[1] E.G. Derouane, Stud. Surf. Sci. Catal. 5 (1980) 5.
[2] M. Guisnet and P. Magnoux, Appl. Catal. A 54 (1989) 1.
[3] S.M. Holmes, A. Garforth, B. Maunders and J. Dwyer, Appl. Catal. A 151 (1997) 355.
[4] M.F. Simpson, J. Wei and S. Sundaresan, Ind. Eng. Chem. Res. 35 (1996) 3861.
[5] W. Zhang and P.G. Smirniotis, Appl. Catal. A 168 (1998) 113.
[6] B. Dimon, P. Cartraud, P. Magnoux and M. Guisnet, Appl. Catal. A 101 (1993) 351.
[7] M. Guisnet and P. Magnoux, Stud. Surf. Sci. Catal. 88 (1994) 53.
[8] L.D. Rollmann and D.E. Walsh, J. Catal. 56 (1979) 139.
[9] M. Bulow, J. Caro and J. Volter, Stud. Surf. Sci. Catal. 34 (1987) 343.
[10] M.A. Uguina, J.L. Satelo, D.P. Serrano and J.I. Valverde, Ind. Eng. Chem. Res. 33 (1994) 26.
[11] F. Niu and H. Hofmann, Appl. Catal. A 128 (1995) 107.
[12] P.G. Smirniotis and W. Zhang, Ind. Eng. Chem. Res. 35 (1996) 3055.
[13] E.J. Rosinski and M.K. Rubin, US Patent 3 832 449 (1974).
[14] F. Ernst, P.A. Jacobs, J.A. Martens and J. Weitkamp, Zeolites 7 (1987) 458.
[15] P.A. Jacobs and J.A. Martens, in: *Proc. 7th Int. Zeolite Conf.* (Kodansha/Elsevier, Tokyo/Amsterdam, 1986) pp. 23–32.
[16] R.B. LaPierre, A.C. Rohrman, J.L. Schlenker, J.D. Wood, M.K. Rubin and W.J. Rohrbaugh, Zeolites 5 (1985) 346.
[17] V.J. Frilette, W.O. Haag and R.M. Lago, J. Catal. 67 (1981) 218.
[18] J. Weitkamp, S. Ernst and C.Y. Chen, Stud. Surf. Sci. Catal. 49 (1989) 1115.
[19] J.L.G. Almedia, M. Dufaux, Y. Ben Taarit and C. Naccache, Appl. Catal. A 114 (1994) 141.
[20] G. Robb, W. Zhang and P.G. Smirniotis, Micropor. Mesopor. Mater. 20 (1998) 307.
[21] W. Zhang, E. Burkle, G. Robb and P.G. Smirniotis, Micropor. Mesopor. Mater. (1999), submitted.
[22] N. Economidis, D. Pena and P.G. Smirniotis, Appl. Catal. B (1999), in press.
[23] C.A. Fyfe, H. Gies, H. Kokotailo, B. Marler and D.E. Cox, J. Phys. Chem. 94 (1990) 3718.
[24] W. Zhang and P.G. Smirniotis, J. Catal. 182 (1999) 400.
[25] W.M. Meier, D.H. Olson and C. Baerlocher, *Atlas of Zeolite Structure Types*, 4th Ed. (Elsevier, London, 1996).
[26] J.M. Newsam, M.M.J. Treacy, W.T. Koestier and C.B. DeGruyter, Proc. Roy. Soc. London A 420 (1988) 375.
[27] E.G. Derouane, in: *Catalysis by Acids and Bases*, eds. B. Imelik, C. Naccache, G. Coudurier, Y. Ben Taarit and J.C. Vedrine (Elsevier, Amsterdam, 1985) p. 221.
[28] A.R. Pradhan, B.S. Rao and V.P. Shiralkar, Stud. Surf. Sci. Catal. 65 (1990) 347.
[29] P.G. Smirniotis and E. Ruckenstein, Appl. Catal. A 117 (1994) 75.
[30] J.M. Newsam, J. Phys. Chem. 93 (1989) 7689.
[31] J. Houzvicka, S. Hansildaar and V. Ponec, J. Catal. 167 (1997) 273.
[32] M. Simon, S.L. Suib and C.L. O'Young, J. Catal. 147 (1994) 484.
[33] W.Q. Xu, Y.Y. Yin, S.L. Suib and C.L. O'Young, J. Catal. 150 (1994) 34.
[34] J. Houzvicka and V. Ponec, J. Catal. 146 (1996) 95.